Environ. Sci. Technol. **2004**, *38,* 139−147

Diversity of Contaminant Reduction Reactions by Zerovalent Iron: Role of the Reductate

ROSEMARIE MIEHR,[†]
PAUL G. TRATNYEK,*[,†]
JOEL Z. BANDSTRA,[†]
MICHELLE M. SCHERER,[‡]
MICHAEL J. ALOWITZ,[‡] AND
ERIC J. BYLASKA[§]

Department of Environmental and Biomolecular Systems, Oregon Health & Science University, 20000 NW Walker Road, Beaverton, Oregon 97006, Department of Civil and Environmental Engineering, University of Iowa, Iowa City, Iowa 52242, and Environmental Molecular Sciences Laboratory, Pacific Northwest National Laboratories, P.O. Box 999, Richland, Washington 99352

The reactions of eight model contaminants with nine types of granular Fe(0) were studied in batch experiments using consistent experimental conditions. The model contaminants (herein referred to as "reductates" because they were reduced by the iron metal) included cations (Cu^{2+}), anions (CrO_4^{2-}, NO_3^-, and 5,5′,7,7′-indigotetrasulfonate), and neutral species (2-chloroacetophenone, 2,4,6-trinitrotoluene, carbon tetrachloride, and trichloroethene). The diversity of this range of reductates offers a uniquely broad perspective on the reactivity of Fe(0). Rate constants for disappearance of the reductates vary over as much as four orders of magnitude for particular reductates (due to differences in the nine types of iron) but differences among the reductates were even larger, ranging over almost seven orders of magnitude. Various ways of summarizing the data all suggest that relative reactivities with Fe(0) vary in the order Cu^{2+}, 5,5′,7,7′-indigotetrasulfonate > 2-chloroacetophenone, 2,4,6-trinitrotoluene > carbon tetrachloride, CrO_4^{2-} > trichloroethene > NO_3^-. Although the reductate has the largest effect on disappearance kinetics, more subtle differences in reactivity due to the type of Fe(0) suggests that removal of CrO_2^{2-} and NO_3^- (the inorganic anions) involves adsorption to oxides on the Fe(0), whereas the disappearance kinetics of all other types of reductants is favored by reduction on comparatively oxide-free metal. Correlation analysis of the disappearance rate constants using descriptors of the reductates calculated by molecular modeling (energies of the lowest unoccupied molecular orbitals, LUMO, highest occupied molecular orbitals, HOMO, and HOMO−LUMO gaps) showed that reactivities generally decrease with increasing E_{LUMO} and increasing E_{GAP} (and, therefore, increasing chemical hardness η).

* Corresponding author phone 503-748-1023; fax: 503-748-1273; e-mail: tratnyek@ese.ogi.edu.
[†] Oregon Health & Science University.
[‡] University of Iowa.
[§] Pacific Northwest National Laboratories.

Introduction

Reduction reactions involving contaminants in the environment are diverse with respect to the environmental compounds that cause reduction and the contaminants that are reduced. Compounds that cause reduction are commonly known as *reductants*, but there is no equally satisfactory term for the compounds that are reduced. Although it is common to refer to chemical agents that are reduced as *oxidants*, this places emphasis on oxidation, which is not intuitive when discussing chemical processes that are characteristic of anoxic, anaerobic, and reducing environments. Instead, we will use a new term, *reductate*, for the chemical compounds that are reduced. The term is consistent with other accepted chemical terminology, e.g., absorbents absorb *absorbates* and eluants elute *eluates*. Thus, reductants reduce reductates (and oxidants oxidize oxidates).

A theme of this manuscript is the diversity of *reductates* that are of environmental interest, particularly those reductates that are important contaminants (or model contaminants). Enough work has been done on the reduction of some classes of reductates to provide a general perspective on their fate. This is, perhaps, most true of the dechlorination of organic compounds, which has been the subject of a number of reviews (e.g., *1*−*3*), but similar reviews are available for the reduction of nitroaromatic compounds (*4*) and transition-metal oxyanions (*5*). In contrast, little work has been done that provides a broad perspective on contaminant reduction reactions across families of reductates (among the few exceptions are refs *6* and *7*). This study provides such a perspective by surveying the reactivity of a wide range of environmentally important reductates, including alkyl halides, nitroaromatics, quinones, metals, and nonmetal inorganics.

In addition to the diversity among reductates, there is diversity among *reductants* that are of environmental interest. Most work in this area has focused on reductants that are important in natural environments, such as ferrous iron (*8*), sulfide (*9*), and natural organic matter (*10*). In the past few years, however, growing interest in applications of zerovalent iron metal, Fe(0), to groundwater remediation has helped to make Fe(0) the most widely studied chemical reductant for environmental applications (*11*). This field has matured so rapidly that some of the most generally significant new insights into environmental reduction reactions have come from studies where Fe(0) was the model reductant, e.g., recognition of the importance of reductive elimination in dechlorination (*12*) and the importance of mass transport in the kinetics of rapid heterogeneous reductions (*13*). Despite these successes, notably little progress has been made toward explaining the variability in reactivity among samples of Fe(0) from different sources. To provide new data on this important problem, this study included granular Fe(0) ranging from the reagent-grade materials used in most laboratory studies to the construction-grade materials used in field-scale applications for groundwater remediation. A future paper will provide additional data and analysis on how the properties of Fe(0) influence its reactivity with reductates.

To address the effects of reductates and reductants simultaneously, we determined the disappearance kinetics for eight model contaminants using nine types of granular Fe(0) under conditions where other experimental variables were as consistent as practical considerations allowed. Surveying all 72 combinations of reductate and reductant precluded detailed investigation of any particular combina-

10.1021/es034237h CCC: $27.50 © 2004 American Chemical Society
Published on Web 11/21/2003

tion, but many of these combinations have been subject to detailed studies previously, and we performed controls or follow-up characterizations where necessary. Kinetic analysis of these data yielded a set of rate constants that were subject to correlation analysis using descriptor variables for the reductates. Descriptors for the reductates were calculated by molecular modeling, and the results are presented in this manuscript. Descriptors for the reductants (i.e., the nine types of granular iron) will be determined by spectroscopic and electrochemical methods, and correlation analysis based on these parameters will be presented in a subsequent publication. Together, the broad perspective afforded by these analyses (i) allows validation and extension of some key generalizations drawn from previous studies, (ii) clarifies the reasons for exceptional behavior where it was observed, and (iii) reveals patterns among classes of reductates that could not have been detected with experimental designs that are more narrow in scope.

Methods

Reagents. The eight reductates investigated were copper sulfate pentahydrate (Spectrum Chemical, Gardena, CA, 98+%), sodium chromate (Fisher Scientific, Pittsburgh, PA, 99+%), potassium nitrate (Aldrich, Milwaukee, WI, 99+%), 5,5′,7,7′-indigotetrasulfonate tetrapotassium salt (TCI America, Portland, OR), 2-chloroacetophenone (Sigma, St. Louis, MO, 99.4%), 2,4,6-trinitrotoluene (Chem Service, West Chester, PA, 99%), carbon tetrachloride (Aldrich, Milwaukee,WI, 99.9 +%), and trichloroethene (Aldrich, Milwaukee,WI, 99.5 +%). Throughout the presentation of results that follows, these reductates will be referred to as Cu2, Cr6, NO3, I4S, 2CAP, TNT, CT, and TCE, respectively.

The nine types of granular Fe(0) used in this study were Aldrich powder (Milwaukee, WI, 97%), Fisher electrolytic powder (Pittsburgh, PA, 99%), EM Science degreased filings (Cherry Hill, NJ), Fluka filings (Milwaukee, WI, 99+%), Baker chips (Phillipsburg, PA, 99.9%), Fisher filings (Pittsburgh, PA, >97%), Master Builders (Cleveland, OH), Peerless Powders and Abrasives (Detroit, MI, "PMP Traditional" Size 8/50, >90%), and Connelly (Chicago, IL, ETI CC-1004, 90%). Throughout the presentation of results that follows, these reductants will be referred to as Ald, Felc, EMS, Flk, Bak, Ffil, MB, PL, and CN, respectively.

To remove fines but minimize other changes, all metal samples were ultrasonicated repeatedly in deionized water until clear supernatants were obtained. The washed iron was then dried by rinsing with methanol during suction filtration, and the resulting material was stored in a vacuum desiccator until used. Only one batch of each type of Fe(0) was prepared, and all analyses were performed with subsamples from these preparations. When not in use, the preparations were stored in a vacuum desiccator. Specific surface areas for the nine preparations, determined by BET N_2 gas adsorption, were Ald, 0.094 $m^2\ g^{-1}$; Felc, 1.27 $m^2\ g^{-1}$; EMS, 0.075 $m^2\ g^{-1}$; Flk, 0.229 $m^2\ g^{-1}$; Bak, 0.040 $m^2\ g^{-1}$; Ffil, 4.09 $m^2\ g^{-1}$; MB, 1.45 $m^2\ g^{-1}$; PL, 1.54 $m^2\ g^{-1}$; and CN, 4.94 $m^2\ g^{-1}$. These values generally fall on the high side of the range of previously reported BET surface areas for these materials (*14*). More detailed characterization of all these Fe(0) preparations will be provided in a subsequent manuscript that focuses on the role of the reductant (Fe(0)).

Batch Experiments. All batch experiments were prepared in an anaerobic chamber (95% N_2/5% H_2 atmosphere) using solutions made from deoxygenated, deionized, unbuffered water. The pH was determined before and after each experiment by opening the container and inserting a glass combination electrode. All experiments were performed at room temperature (~23 °C).

Cu2 and Cr6 disappearance kinetics were determined in 40 mL VOA vials containing 0.1−8.0 g of Fe(0) for Cu2 and 3.0 g of Fe(0) for Cr6. The vials were filled with 0.2 M Cu2 or 0.5 mM Cr6 and sealed with polypropylene screw caps with TFE-lined silicone septa prior to removal from the anaerobic chamber. During incubation, the vials were mixed at 40 rpm on a rotator with the plane in vertical orientation (i.e., end-over-end). Periodically, 0.4-mL aliquots were removed, filtered through a 0.45 μm 4-mm nylon syringe filter, and placed in a 1 cm cuvette for measurement of absorbance by UV−vis spectrophotometry. The filtered samples containing Cu2 were diluted 10-fold (to keep absorbance readings below 1 AU) with deionized water. In the case of Cr6, the samples were diluted 10-fold with pH 10 carbonate buffer (to stabilize the speciation of Cr6 as CrO_4^{2-}). Concentrations were quantified at the respective absorbance maxima (λ_{max} = 813 nm for $CuSO_4$ and 372 nm for K_2CrO_4).

NO3 reduction kinetics were measured in 125-mL glass serum bottles containing 3.0 g of Fe(0) and 120 mL of 0.49 mM KNO_3.The filled bottles were crimp-sealed with Hycar septa (Pierce, Rockford, IL) and then removed from the anaerobic chamber for incubation and analysis. During incubation, the bottles were mixed at 40 rpm on a rotator with the plane oriented 60° from horizontal. Periodically, 1 mL samples were withdrawn via the septum through 0.2 μm nylon syringe tip filters (Alltech Deerfield, IL). The filtrate was analyzed for nitrate by ion chromatography as described previously (*14*).

I4S reduction studies were carried out in 4 mL screw-cap quartz cuvettes (Starna Cells, Atascadero, CA). A 0.02−3.0 g amount of Fe(0) was added to the cuvette, which was then transferred into the glovebox, filled with 4 mL of I4S solution (0.07 mM), and sealed with a screw cap that was lined with a Teflon-lined butyl rubber septa (Wheaton, Millville, NJ). Outside the glovebox, the decrease in concentration of the oxidized form of I4S (λ_{max} = 519 nm) was monitored continuously using the time-drive capability of the spectrophotometer (Perkin-Elmer, Lambda 20). About once every 30 s, the measurement was interrupted to mix the contents of the cuvette (inverting once by hand). Validation of this method for a range of redox indicators was described previously (*15*).

2CAP reductions were carried out in 60 mL glass serum bottles containing 1.0−9.0 g of Fe(0). The serum bottles were completely filled with 100 μM 2CAP, crimp-sealed using butyl rubber septa (Pierce, Rockford, IL), and removed from the anaerobic chamber. During incubation, the bottles were mixed at 40 rpm on a rotator with the plane oriented 85° from horizontal. Periodically, 0.4 mL samples were withdrawn via the septum and filtered through a 0.45 μm Nalgene 4 mm nylon syringe filter. The concentrations of 2CAP and its reduction products were determined by high-performance liquid chromatography (HPLC) using an Econosil (Alltech, Deerfield, IL) C18 column (250 mm × 4.6 mm i.d.) and UV detection at 210 nm. The mobile phase consisted of 45/55 acetonitrile/water with a flow rate of 1 mL min^{-1}.

TNT reduction was investigated using 40 mL VOA vials containing 0.5−8.0 g of Fe(0). After filling the vials with 176 μM TNT solution, the samples were mixed at 40 rpm on a rotator with the plane oriented 85° from horizontal. Periodically, 0.2 mL samples were withdrawn and analyzed immediately by HPLC. Analytical conditions were the same as described above for 2CAP, except that absorbance of TNT and its degradation products were monitored at 254 nm. TNT and some degradation products (2- and 4-aminodinitrotoluene, 2,4- and 2,6-diaminonitrotoluene) were identified and quantified by comparison with commercial standards.

CT and TCE reduction was studied by batch methods similar to those used previously in this laboratory (e.g., *16*). In the glovebox, 10 mL serum vials containing 1.0 g of Fe(0) for the CT experiments or 1.0, 2.0, or 0.5 g for TCE experiments were filled with deionized water (leaving no headspace) and

crimp-sealed with Hycar septa. Spiking with 60 or 120 μL aliquots of saturated TCE solution or 100 μL of saturated CT solution gave initial concentrations of 45 μM for CT and 42 or 84 μM for TCE. Separate vials for each time point were prepared at once, and all vials were mixed together at 40 rpm on a rotator with the plane oriented 85° from horizontal. Periodically, a vial was sacrificed for analysis by removing the septum and transferring 1 mL for extraction with 1 mL of hexane. The hexane extracts were analyzed by gas chromatography using a DB 624 (J&W, Folsom, CA) column (30 m × 0.53 mm i.d. with 3 μm film thickness) and ECD detection. Controls without iron were run to determine losses due to volatilization.

Molecular Modeling. Hartree−Fock (HF) and density functional theory (DFT) calculations were performed using the NWChem, version 4.0, program suite (*17*) and Gaussian-98 program suites (*18*). The HF calculations were done using the augmented polarized double-ζ 6-31+G* basis set (*19*−*22*). The DFT calculations were solved using the B3LYP exchange-correlation functionals (*23, 24*) with the polarized double-ζ DZVP2 basis set (*25*).

Solvent effects were estimated using the self-consistent reaction field theory of Klamt and Schüürmann (COSMO) (*26*), with the cavity defined by van der Waal's radii or the united atom model (*27*). COSMO theory can be combined with a variety of ab initio electronic structure routines, including HF and DFT with the B3LYP functional. The calculated gas-phase geometries were used in the solvation calculations.

Results and Discussion

General Kinetic Considerations. The raw kinetic data are presented as a matrix of log-concentration versus time plots as Supporting Information (Figure S1). Each cell in this matrix represents a combination of reductate and reductant and shows all of the time courses that were used in subsequent kinetic analyses. In some cases, multiple time courses represent replicates, but in other cases they result from varying the amount of Fe(0) or the amount of reductate used in each experiment. In general, each time course presents a smooth disappearance curve defined by about 20 points (n ranges from 6 to 100), without significant noise or individual outliers.

The semilog plots of these disappearance curves (Supporting Information, Figure S1) suggest kinetics that are predominantly first order in reductate concentration, but a variety of deviations from pseudo-first-order behavior are also evident. These deviations have been seen in previously reported studies of contaminant reduction by Fe(0), and most have been explained and modeled. Gradual convexities typically reflect a transition from kinetics that are limited by availability of reactive sites to kinetics limited by reaction at occupied sites (*28, 29*). However, sharper breaks (lags) would arise, for example, if rapid contaminant reduction occurred only after autoreduction of the passive film on the Fe(0) particles (*30*). Sharp concavities may be due to rapid adsorption preceding slower transformation reactions (*31*−*33*), but gradual concavities (tails) are usually due to changes in the system pH or accumulation of reaction products (*34*−*37*). Among the deviations from first-order behavior that are evident in the data from this study, the most significant cases are discussed below in the sections on individual reductates.

To achieve the goals of this study, it was necessary to reduce all of the kinetic data to a set of comparable rate constants without misrepresenting the main processes controlling the disappearance kinetics of any reductate. Where previously reported kinetic studies were available for individual reductates, we used their conclusions to help decide how to fit the data from this study. We then fit all of our data for a particular reductate in a consistent fashion. Specifics regarding the data analysis for each reductate are provided in the sections that follow. In every case, the data were eventually reduced to a pseudo-first-order rate constant, k_{obs}. These values were then used to obtain a surface-area-normalized rate constant, k_{SA}, by dividing k_{obs} with the appropriate surface area concentration of Fe(0), as described previously (*34*). The resulting values of k_{obs} and k_{SA} are tabulated as Supporting Information (Table S1). Other experimental results (major products identified and pH before and after reaction) are also included in Table S1.

Individual Reductates. *Cu2.* The process of removing cupric ion (Cu2) from water with Fe(0) has been described in the literature on cementation (*38, 39*). In the presence of high Cu2 concentrations, the reduction of Cu(II) to Cu(0) by Fe(0) results in plating of copper metal onto the iron surface. Under appropriate conditions, the plating process can be very sensitive to impurities, roughness, and other irregularities of the metal surface. Because the uniformity of the film of metallic copper can be characterized by visual inspection, various procedures involving exposing metal samples to solutions of Cu2 have long been used for quality control in the metal finishing industries (*40*).

The precipitation of Cu(0) also leads to decolorization of the solution. Because this process is easy to monitor visually and spectrophotometrically, it has been suggested that decolorization of $CuSO_4$ solution might provide a method to screen samples of granular Fe(0) for reactivity prior to application in remediation of groundwater. Interpreting the results of this test, however, is likely to be difficult because the chemistry of plating copper onto iron is profoundly different than the chemistry that makes Fe(0) effective at removing contaminants such as TCE and chromate. To investigate how Cu2 compares to other reductates, it was selected as one of the reductates used in this study over other divalent metals—such as Pb(II), Cd(II), Ni(II), and Hg(II)—that also can be removed from water by cementation with Fe(0) (*41*).

Immediately after addition of $CuSO_4$, all nine types of iron began to develop the orange color suggestive of the formation of Cu(0). Visual inspection showed that the fine-grained iron samples were completely covered with Cu(0) by the end of a typical experiment, and the coarse-grained samples of iron were mostly covered. Because the plating of Cu(0) progressively covers the Fe(0) surface, we assumed that initial Cu2 disappearance data would be most representative of the kinetics of reaction with Fe(0).

A variety of control experiments were performed to determine what processes were responsible for the kinetic profile observed for Cu(II) disappearance. Decolorization of the solution occurred more rapidly with more aggressive mixing (data not shown), suggesting that mass transport was influential during the initial—apparently first order—phase of the reaction. Previous work on the cementation of Cu(II) by Fe(0) also found that Cu(II) disappearance was first order but affected by mass transport (*38*, *39*). For quantitative analysis in this study, we calculated k_{obs} from our initial rate data, and the resulting rate constants are tabulated as Supporting Information (Table S1).

Cr6. A variety of hazardous metal oxyanions—including chromate, pertechnetate, uranyl, arsenate, and selenate—can be removed from water with Fe(0) (*41*). Among these reductates, the chemistry of chromate (Cr6) removal by Fe(0) was the first to be studied in detail, so it was used in this study. The process of Cr6 removal is complex and apparently involves adsorption of Cr6 to the iron oxides associated with Fe(0) and reduction of Cr6 to Cr(III) followed by coprecipitation of Fe(II/III)/Cr(III) oxyhydroxides (*42*−*44*). The combination of these processes results in disappearance kinetics that are sufficiently fast that the kinetics of Cr6 removal by granular Fe(0) may be influenced by mass transport (*14*, *45*).

SCHEME 1

Indigo-5,5',7,7'-tetrasulfonate (I4S)

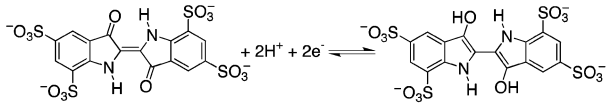

In this study, the kinetic data for disappearance of Cr6 suggest a relatively slow first-order process for the Fe(0) samples with minimal oxide (Ald, Felc, Flk, Bak), which generally produced final pH values around 8. In contrast, the Fe(0) samples that include larger amounts of oxide (Ffil, MB, PL, CN) produced higher final pH values (ca. 10) and Cr6 disappearance kinetics with pronounced tailing. Therefore, we described the kinetics of Cr6 reduction with first-order rate constants calculated using all data except those associated with the tails. Overall, this treatment is consistent with the more detailed study of Cr6 reduction kinetics by Alowitz et al. (*14*), where they interpreted their data as first-order disappearance kinetics with greater tailing at higher pH due to precipitation of Fe(II/III)/Cr(III) oxyhydroxides.

NO3. Abiotic reduction of nitrate (NO3) by Fe(0) produces NH_4^+ as the main product, although small amounts of NO_2^- have been observed under some conditions (*14, 46*−*50*). The kinetics of NO3 reduction by Fe(0) are relatively slow (*14*), so our experiments with NO3 were run longer than other reductates included in this study. Despite this fact, the extent of reaction achieved was only about one-half of the initial NO3 concentration, which precluded unambiguous determination of the reaction order from our data. More detailed studies of NO3 reduction by Fe(0) found similarly slow kinetics at pH values near-neutral or above but showed that NO3 disappearance is demonstrably first-order at pH 5−6 where the reaction is faster (*14, 47, 48, 51, 52*). Therefore, we assumed pseudo-first-order kinetics for the NO3 disappearance data obtained in this study and fit all but the first few points to obtain k_{obs} for further analysis. The few data that were excluded formed short segments of steep slope at the beginning of experiments with all types of Fe(0) except EMS. This effect has been noted previously in unbuffered systems and is most likely due to the rapid increase in pH immediately after the unbuffered medium is contacted with Fe(0) (*14, 47, 48*).

I4S. The various sulfonated forms of indigo (di, tri, and tetra) have long been used as redox indicators (*53*). Their high solubility makes them less prone to adsorption in heterogeneous environmental media (*54*), and their Nernstian redox behavior makes them useful as model mediators of electron transfer (*55*). The redox couples formed by the various indigo sulfonates involve a conjugated system analogous to quinone/hydroquinone couples (Scheme 1). Both systems presumably react with Fe(0) by two sets of single electron-transfer and protonation steps divided by a semiquinone radical intermediate. One reason that we chose to study indigo tetrasulfonate (I4S), rather than a more well-known quinone such as anthraquinone disulfonate (AQDS), is that the pronounced color change exhibited by I4S (blue to yellow) makes it a possible alternative to Cu2 as an indicator for screening the relative reactivities of various samples of Fe(0).

Good mass balance during reduction of I4S by Fe(0) has been demonstrated previously by measurement of absorbance I4S and its reduced form at their respective λ_{max} values (*15*). In this study, we used continuous measurement of I4S absorbance in a sealed cuvette to efficiently obtain kinetic data that was free from any reoxidation of the reduced I4S by adventitious O2. The data still exhibit tailing because the reaction was monitored nearly to completion (*15*), and these points were excluded from further kinetic analysis. More notable is the suggestion of a lag in the data, most notably with four of the reagent-grade Fe(0) samples (Ald, Felc, Flk, and Bak). Follow-up experiments (not shown) performed with Ald and Felc demonstrated that the lag was eliminated by allowing as little as 10 min of equilibration between the Fe(0) and water before adding the I4S. Excluding data assigned to tails and lags left data that was satisfactorily fit as pseudo-first-order, and the resulting rates constants are tabulated as Supporting Information (Table S1).

Unlike the other eight types of Fe(0) studied, EMS appeared unreactive with I4S during preliminary experiments, so larger amounts of EMS iron were needed to produce the disappearance shown in the Supporting Information (Figure S1). We hypothesized that this anomalous behavior of EMS was an effect of pH because EMS gave solutions with pH values that were higher than the other Fe(0) samples (see Supporting Information, Table S1). In support of this hypothesis, we note that adjusting the solution generated by contact with EMS down to pH 7 resulted in more rapid reduction of the I4S and raising the pH generated by Ald from 7 to 10 resulted in much slower reduction of I4S (data not shown).

2CAP. 2-Chloroacetophenone is of interest primarily due to its utility as a probe substance for distinguishing between reduction by electron-transfer and hydride transfer mechanisms (*56*). As shown in Scheme 2, reduction by electron transfer produces acetophenone and hydride transfer produces 2-chlorophenylethanol, either of which can be further reduced to *sec*-phenyl ethanol. The reduction of contaminants by Fe(0) is generally considered to be an electron-transfer process (*16*), although possible roles for hydrogen-atom transfer (*16, 57*−*59*), and even hydride transfer (*60, 61*) have been discussed. In addition to clarifying whether hydride transfer occurs in these systems, the kinetic data obtained with 2CAP is of interest because it involves a chlorinated alkane with "substituents" that are very different than those whose reaction with Fe(0) has been studied previously (e.g., 1,1,1-trichloroethane (*29, 62*) and DDT (*63*)).

The reduction of 2CAP by eight types of iron metal (all of those tested except EMS) produced acetophenone as the only detectable product. Initially, appearance of acetophenone was sufficient to define mass balance, which suggests that reduction of 2CAP by Fe(0) occurs predominantly by electron transfer and that hydride plays a negligible role. By the end of most experiments, identifiable products decreased to 75−90% of the 2CAP lost, suggesting that further reaction by adsorption and/or transformation to other products does eventually become significant.

The strongest evidence for an unidentified transformation pathway was obtained with EMS iron, which gave rapid disappearance of 2CAP but no evidence for any of the expected reduction products that are shown in Scheme 2. Because EMS produces a distinctly higher final pH than the other samples of Fe(0) and 2-hydroxyacetophenone was identified as the major product, we hypothesized that the reaction of 2CAP with EMS iron was due to base-catalyzed hydrolysis. To test this, we exposed 2CAP to Ald with the initial pH adjusted up to 10, and this experiment produced primarily 2-hydroxyacetophenone (data not shown), as expected if hydrolysis of 2CAP to 2-hydroxyacetophenone superseded reduction at high pH.

The shape of the log-concentration vs time plots for 2CAP disappearance exhibited little evidence for tailing but occasional evidence for lags (Felc and Flk) and convexity (Ald, Felc, CN). As with the other reductates that gave lags (I4S and TNT), this effect was noted mainly with reagent-grade Fe(0) and could be eliminated by equilibrating the Fe(0) with water for a brief period prior to adding 2CAP. Convex log-concentration vs time plots can arise from kinetics that are transitional from zero- to first-order as reductate disappearance evolves from site-limited to reaction-limited

SCHEME 2

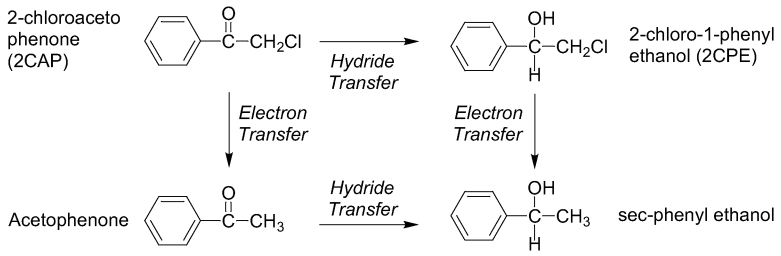

kinetics (*28, 29*). Such data can be fit directly to a mixed-order model with separate terms for the maximum rate of reaction, V_{max}, and concentration of reductate at one-half of V_{max}, $K_{1/2}$. An advantage of this approach is that all of the data in a mixed-order disappearance curve can be fit to a single model. Then, the fitted parameters can then be used to calculate $V_{max}/K_{1/2}$, which is directly comparable to k_{obs} (*29*). For all the 2CAP data used later in this study, we used $V_{max}/K_{1/2}$ to calculate k_{obs} and k_{obs} to calculate k_{SA}.

TNT. Trinitrotoluene and other nitroaromatic compounds react rapidly with Fe(0) in conventional batch experiments to give a variety of nitroso, hydroxylamino, amino, and conjugation products (*64*−*68*). In this study, eight types of iron metal (all of those tested except EMS) produced mixtures of products that included 2- and 4-aminodinitrotoluene (ADNT), 2,4- and 2,6-diaminonitrotoluene (DANT), and several unidentified peaks. The identifiable products accounted for only a few percent of the TNT lost, and the unidentified putative product peaks were not large enough to account for the missing mass (assuming all products are substituted benzenes and have roughly similar response factors). Therefore, it is likely that a substantial portion of the unrecovered TNT and nitro reduction products were adsorbed or otherwise bound to the iron (*68*). In contrast to the pattern of reactivity observed with TNT and most of the iron types tested, EMS produced very little disappearance of TNT and no evidence for appearance of products, even after 2 days of exposure.

The kinetic data for disappearance of TNT showed complexities similar to those obtained with the other two aromatic reductates (I4S and 2CAP). A lag was noted with Felc (and perhaps Flk), and variable degrees of convexity in log-concentration vs time plots were found for Felc, Flk, Bak, Ffil, PL, and CN. In addition, Ald and MB iron gave initial losses of TNT that seemed most consistent with rapid adsorption, also noted below for TCE. After omitting the data associated with lags and adsorption, the rest were fit to pseudo-first-order or mixed-order kinetics, as appropriate. The resulting values of k_{obs} and k_{SA} for TNT, which are used in the analysis that follows, were first reported in ref *67* along with additional kinetic data and validation of analysis.

CT. Numerous studies have shown that the major pathway for reduction of carbon tetrachloride by Fe(0) is hydrogenolysis to produce chloroform (e.g., *16, 69, 70*). In addition, variable amounts of CT apparently react by a minor pathway that produces formate and/or CO via hydrolysis of the dichlorocarbene intermediate (*70*). The kinetics of CT disappearance due to reaction with Fe(0) are faster than most other chlorinated solvents (*34, 71*) but not so fast that mass transport is likely to influence the observed rate of reaction (*72*).

Eight of the iron types tested (all but EMS) reduced CT rapidly, with chloroform as the major product. As with TNT, EMS was unique in that it gave little if any reduction of CT. The four Fe(0) samples that seem to have the most oxide (Ffil, MB, PL, and CN) gave smooth first-order disappearance of CT, with variable but small amounts of tailing after 300 min of contact time. Flk and Ald also gave first-order disappearance of CT, although the time course for Ald suggests a lag and a tail, and these data were omitted from further analysis. Reaction with Felc, Bak, and EMS was too slow to give distinguishing features, and the data were assumed to be first-order.

TCE. Under most conditions, the major pathway for reaction of trichloroethylene with Fe(0) is reductive β-elimination to give chloroacetylene (*12, 73*). The kinetics of TCE reduction by Fe(0) are inhibited by intra- and inter-adsorbate competition for surface sites, and these effects have been described with variations on the Langmuir−Hinshelwood−Hougen−Watson (LHHW) kinetic model (*12*). The LHHW model is similar in form to the mixed-order kinetic model that was used in this study to fit some of the disappearance data for 2CAP and TNT.

As expected, TCE proved to be the least reactive of all the organic reductates included in this study. Because a similar design was used for experiments with all the reductates, the extent of reaction obtained for TCE was rather small (ca. one half-life). Under these circumstances, small amounts of the expected products from TCE degradation by Fe(0) would not have been detectable with the analytical methods we used. However, most of the kinetic data for disappearance of TCE (Supporting Information, Figure S1) showed a common pattern of rapid initial loss (presumably due to adsorption (*31*−*33*)) followed by gradual disappearance that suggested first-order reduction. We fit only the latter portion of the data to obtain the rate constants used in this study.

Trends Among the Reductates. Qualitative Trends and Groups. Figure 1 summarizes our values of k_{SA} for each combination of reductate (rows) and reductant (columns). This figure helps put the differences among the data into context. For example, where duplicate (or in two cases, triplicate) values of k_{SA} are available for a particular combination of reductate and reductant, the data appear as concentric circles only if there is a significant difference between the results. Figure 1 reveals no significant differences between duplicates where the same amount of Fe(0) was used (i.e., replicates). Where the duplicates represent experiments performed with different amounts of Fe(0), they serve to test the assumption that the linear model for calculation of k_{SA} is adequate to normalize for differences in surface area concentration. Figure 1 reveals only a few cases where duplicate values of k_{SA} differ significantly (e.g., I4S-EMS and TNT-Bak), and there is no pattern in these occurrences to suggest that they arise due to a systematic influence on the experimental results. Thus, the variability in replicates apparently reflects only indeterminant error, and this error is small relative to the overall range in k_{SA} for all reductates and types of Fe(0).

The comprehensive perspective provided by Figure 1 reveals several broad trends in the data. Most apparent is that differences among the reductates are more pronounced than differences among the types of Fe(0). Thus, it should be possible to make generalizations about the relative reactivity of the various reductates without regard to Fe(0) type. In contrast, generalizations regarding the relative reactivity of the various types of Fe(0) may require parameters that incorporate the effect of reductate structure on reactivity.

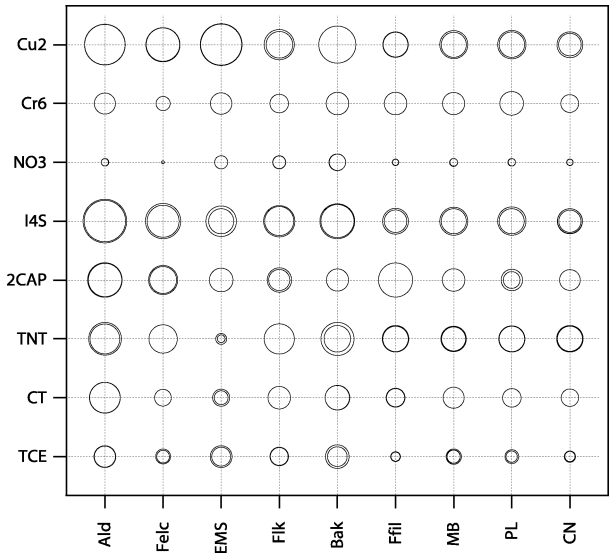

FIGURE 1. Bubble plot of all rate constants (log k_{SA}) represented as ring size, plotted versus reductate (ordinate) and reductant (abcissa). All experiments are represented by rings in this figure, but most appear as a single ring. Intermediate differences among replicate experiments create overlapping rings which appear thicker.

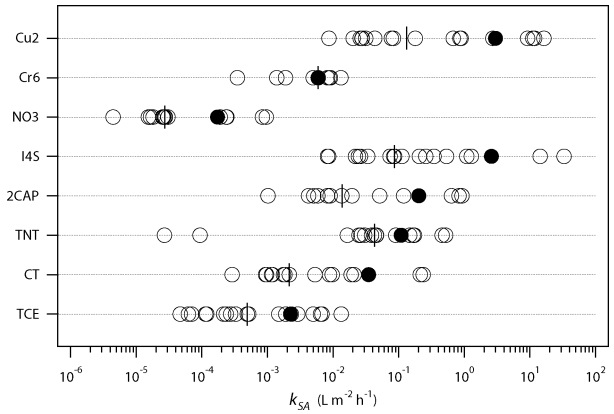

FIGURE 2. Dot plot of all rate constants (k_{SA}) plotted versus reductate (ordinate). Open circles represent individual experiments; solid circles represent arithmetic mean, and vertical bars represent the median of individual values for each reductate. Data for the mean and median values are given in Table 1.

The bulk of the remainder of this paper is about the effects of the reductates, and the effects of Fe(0) type will be the focus of a future paper.

Figure 2 shows individual and mean values of k_{SA} for each reductate. Medians are also shown as an alternative measure of central tendency. (The mean and median values of k_{SA} are given in Table 1.) Although there is considerable scatter among the individual values for each reductate—mostly due to the effects of Fe(0)—the differences among the reductates are larger. From inspection of Figure 2, it is apparent that rates of reduction by Fe(0) generally follow the order Cu2, I4S > 2CAP, TNT > CT, Cr6 > TCE > NO3. Looking back at Figure 1, the same trend is apparent by comparing the relative sizes of the circles among rows, even though the trend is not always consistent for a particular Fe(0) (i.e., within columns in Figure 1). This ranking of relative reactivities, over such a diverse range of reductates, provides an expanded perspective on the reactivity of Fe(0). Therefore, it is of interest to validate the generality of this ranking by comparing it to previously reported values of k_{SA}, where appropriately data are available.

TABLE 1. Representative Rate Constants by Reductate

reductate	abbr.	median k_{SA}[a]	mean k_{SA}[a]	1 S.D.	*n*
cupric	Cu2	1.32E-01	2.99E-0	5.18E-0	18
chromate	Cr6	5.89E-03	5.97E-3	4.24E-3	9
nitrate	NO3	2.71E-05	1.73E-4	2.88E-4	17
indigo tetrasulfonate	I4S	8.50E-02	2.58E-0	7.85E-0	20
2-chloroacetophenone	2CAP	1.37E-02	2.02E-1	3.45E-0	13
2,4,6-trinitrotoluene	TNT	4.27E-02	1.09E-1	1.53E-0	17
carbon tetrachloride	CT	2.16E-03	3.48E-2	7.73E-2	15
trichloroethene	TCE	4.96E-04	2.24E-3	3.44E-3	19

[a] k_{SA} in L m^{-2} h^{-1}.

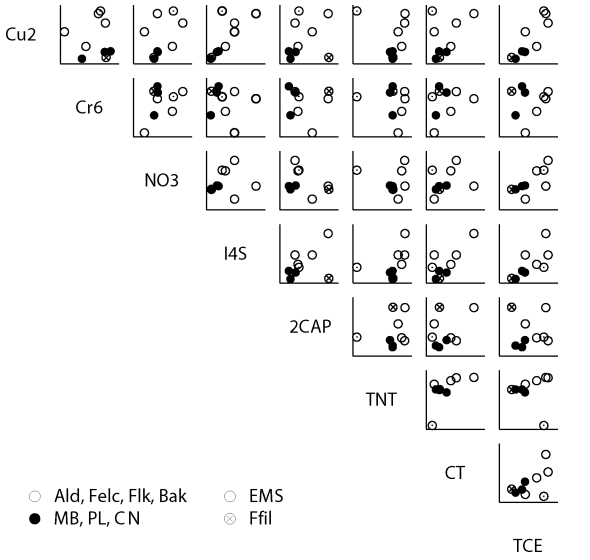

FIGURE 3. Scatter plot matrix of average rate constants (log k_{SA}) for all combinations of reductates. Each point in each plot represents one of the nine types of Fe(0) studied.

For chlorinated aliphatic compounds, the average k_{SA}'s reported by Johnson et al. (*34*) are of particular relevance because they are based on results that include a range of Fe(0) types. For TCE, Johnson et al. found an average $k_{SA} = 3.9 \times 10^{-4}$ L m^{-2} h^{-1}, which is 10-fold below the average but well within the range of values obtained in this study. For CT, Johnson et al. found an average $k_{SA} = 1.2 \times 10^{-1}$ L m^{-2} h^{-1}, which is 3-fold above the average but also within the range of results found in this study. For TNT, we have shown previously that the data from this study fall within the range of reported rate constants for reaction of nitroaromatic compounds by Fe(0) (*67*). Much less kinetic data has been reported for the other reductates. Using buffered media and Ffil, k_{SA}'s for NO3 and Cr6 were found to be a function of pH (*14*). Over pH 7–9, k_{SA} decreased sharply from 1.3×10^{-3} to 8.0×10^{-5} L m^{-2} h^{-1} for NO3, and for Cr6 three types of Fe(0) gave an average k_{SA} of 2.1×10^{-1} L m^{-2} h^{-1} (for pH 7). These values of k_{SA} agree reasonably well with the values obtained in this study. For I4S, the only value of k_{SA} that has been reported previously is 0.23 L m^{-2} h^{-1} (*15*), which falls at the median of values obtained in this study.

Figure 3 shows correlations among k_{SA}'s for all combinations of the reductates. Where duplicate values of k_{SA} were available for a reductate–reductant combination, the average value was used, so the plots in the matrix include only one point for each type of Fe(0). The main goal of Figure 3 is to reveal any correlations between reductates that might have

diagnostic or predictive value. Interestingly, the most prominent correlation is Cu vs TCE ($r^2 = 0.76$), which—as we noted above—would seem unlikely due to differences in the ways that these two reductates react with Fe(0). Excluding one anomalous point reveals several other good correlations. The low value of k_{SA} for EMS−TNT distorts all of the plots involving TNT, but the remaining eight points give strong correlations for TNT vs TCE ($r^2 = 0.78$) and vs Cu2 ($r^2 = 0.72$). Other correlations of possible interest include Cu2 vs I4S without EMS ($r^2 = 0.94$) and I4S vs 2CAP without Ffil ($r^2 = 0.77$).

Encoding the symbols in Figure 3 to represent different types of Fe(0) reveals two additional trends in the data. First, construction-grade Fe(0) (MB, PL, and CN) and the one reagent-grade Fe(0) that contained similarly large amounts of oxide (Ffil) tend to plot in a tight cluster relative to the reagent-grade Fe(0) with low amounts of oxide (Ald, Felc, Flk, Bak, and EMS). Furthermore, the cluster of points representing Fe(0) that is high in oxide falls near the origin of most plots, reflecting relatively low values of k_{SA}. This is true for all the reductates except Cr6, where the cluster of points for high-oxide Fe(0) plots opposite the origin, reflecting relatively large values of k_{SA}, and NO3 where the cluster of high-oxide data exhibits intermediate behavior. Because Cr6 and NO3 are the only inorganic anions among the reductates studied, it appears that the disappearance kinetics of these reductates is favored—and at least partly controlled—by adsorption to oxides on the Fe(0). In contrast, the disappearance kinetics of all other types of reductants seems to be more rapid with Fe(0) that is comparatively free of oxides, suggesting that reduction by the metal is at least partially rate determining.

Correlation Analysis. The ordinal ranking of reductate reactivities that was obtained from Figure 2 would be of greater value if it could be described by a continuous numerical function that relates k_{SA} to descriptor variables that are applicable to all the reductates of interest. The identification of such relationships is typically done by correlation analysis (*74*), and a successful correlation analysis might lead to quantitative structure−activity relationships (QSARs) that could be used to predict values of k_{SA} of reductates for which kinetic data are not available.

For small training sets of closely related reductates (e.g., chlorinated ethenes), it is often not difficult to find descriptor variables that give acceptable QSARs for contaminant reduction reactions (*75*). However, more diverse data sets create a number of issues that make correlation analysis difficult (as exemplified by the three contrasting approaches taken to correlation analysis of one set of k_{SA}'s for chlorinated methanes, ethanes, and ethenes (*71*, *76*, *77*)). In this study, the training set of reductates extends beyond dechlorination, which places further constraints on the range of applicable descriptor variables and the types of conclusions that can be drawn from the resulting correlations (*74*, *75*).

The constraints on descriptor selection are both practical (i.e., the descriptor must be measurable or calculable for all reductates) and theoretical (i.e., it must represent a reductate property with some plausible bearing on the rate-limiting step of the reaction). For the present case, these criteria are met by the energy of the lowest unoccupied molecular orbital of the reductates (E_{LUMO}). E_{LUMO} has been used frequently as a descriptor variable in correlation of reduction rate constants, and the strengths and limitations of this approach have been discussed from various perspectives (*71*, *75*, *77*, *78*). One alternative to E_{LUMO} is the (vertical or adiabatic) electron affinity, which should be a more precise descriptor of reduction reactions where the rate-limiting step is simply electron attachment (to form a radical anion). Another alternative to E_{LUMO} is the difference between the E_{LUMO} and the energy of the highest occupied molecular orbital (E_{HOMO}), i.e., the HOMO−LUMO energy gap (E_{GAP}). E_{GAP} is sometimes

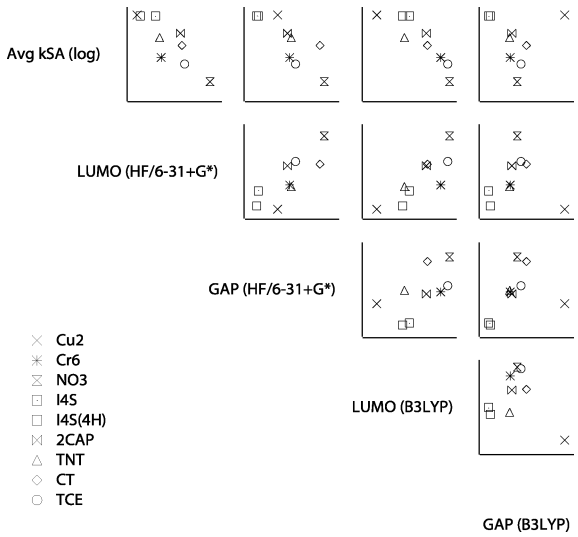

FIGURE 4. Scatter plot matrix of average rate constants (log k_{SA}) and selected molecular descriptors. The molecular descriptors shown include the E_{LUMO} and E_{GAP} calculated using HF/6-31+G* and B3LYP, with solvation using the COSMO model. Data for k_{SA} are given in Table 1, and E_{LUMO} and E_{GAP} are tabulated in Table S2 of the Supporting Information.

regarded as a general index of reactivity (*79*) and is directly proportional to the absolute hardness, η (*80*).

$$\eta = (E_{LUMO} - E_{HOMO})/2 \quad (1)$$

Hardness can be understood as the resistance of a molecule to change in its electron density distribution (*81*). Thus, hard molecules (which have large E_{GAP}'s) offer more resistance to electron transfer and therefore might be less reactive with Fe(0). E_{GAP} and η were of particular interest in this study because they offer comparatively general descriptors of reactivity, which might be more effective in correlation analysis of data where considerable diversity in reduction mechanisms is expected.

For use in this study, we calculated E_{LUMO}, E_{HOMO}, and E_{GAP} for the eight reductates (plus the fully protonated form of I4S) with a variety of theoretical models and have included the most reliable and complete results as Supporting Information (Table S2). Figure 4 shows correlation plots for the average values of k_{SA} and all combinations of the two descriptors (E_{LUMO} and E_{GAP}) calculated at two levels of theory (HF/6-31+G* and B3LYP/DZVP2) with solvation using the COSMO Model. Other levels of theory, types of solvation model, and modeling packages gave similar values of E_{LUMO} and E_{GAP} (Supporting Information, Figure S2). The first row in Figure 4 shows that k_{SA} correlates remarkably well with the E_{LUMO} obtained by HF/6-31+G* and B3LYP/DZVP2 ($r^2 = 0.68$ with HF/6-31+G* and $r^2 = 0.77$ with B3LYP/DZVP2), and the trend in reactivity is as expected: k_{SA} decreases with increasing E_{LUMO}. The correlation with E_{GAP} is somewhat more complex. The HF/6-31+G* calculated values of E_{GAP} give favorable correlations ($r^2 = 0.61$), and the trend in reactivity again as expected: k_{SA} decreases with increasing E_{GAP} (and, therefore, increasing η). On the other hand, the B3LYP/DZVP2 calculations do not show a good correlation between k_{SA} and E_{GAP}, due mainly to the large E_{GAP} for Cu2 obtained by B3LYP/DZVP2. From Figure S2 (Supporting Information) it is apparent that the large E_{GAP} for Cu2 arises from reproducible differences in the E_{HOMO} obtained from the two levels of theory.

Recognizing that there is no a priori reason to expect a simple correlation for all of the reductates included in this study, we believe that the correlations shown in Figure 4 are

remarkably good, and selecting one correlation over another based on modest differences in the statistics is not likely to be chemically meaningful. However, because it was concluded previously—based on the analysis of Figure 3—that the k_{SA}'s for NO3 and Cr6 were influenced by adsorption and some of the correlations shown in Figure 4 are leveraged strongly by the point for NO3, it is of interest to consider how the kinetic data correlate to E_{LUMO} and E_{GAP} without these values. Excluding NO3 and Cr6 from the correlation has no effect on the general trends in reactivity and makes little difference to the statistics (e.g., for HF/6-31+G*, $r^2 = 0.67$ with E_{LUMO} and $r^2 = 0.50$ with E_{GAP}). Rather than removing ad hoc outliers from among the reductates, a more promising approach to improving the correlations obtained with the data from this study is to remove the variation in k_{SA} due to the different types of Fe(0). However, this analysis calls for the development of a descriptor variable for the role of the Fe(0), which will require a more detailed characterization of the properties of the Fe(0) used in this study. These issues will be developed in a future manuscript, utilizing the same kinetic data described here but with emphasis on the role of the reductant (i.e., the iron) in determining the reaction kinetics.

Acknowledgments

This work was supported by the U.S. Environmental Protection Agency (Cooperative Agreements CR 82078-01-0 and R827117), the Strategic Environmental Research and Development Program (SERDP, Projects CU-1176 and CU-1232), and the National Science Foundation (BES-9983719). This report has not been subject to review by any of the agencies and therefore does not necessarily reflect their views, and no official endorsement should be inferred.

Supporting Information Available

Reaction notes (pH and products), rate constants (k_{obs} and k_{SA}), reductate descriptors (E_{HOMO} and E_{LUMO}, and E_{GAP}) are tabulated as Supporting Information. This material is available free of charge via the Internet at http://pubs.acs.org.

Literature Cited

(1) Vogel, T. M.; Criddle, C. S.; McCarty, P. L. *Environ. Sci. Technol.* **1987**, *21*, 722−736.
(2) Baxter, R. M. *Water Poll. Res. J. Canada* **1989**, *24*, 299−322.
(3) Reinhard, M.; Curtis, G. P.; Barbash, J. E. In *Subsurface Restoration*; Ward, C. H., Cherry, J. A., Scalf, M. R., Eds.; Ann Arbor: Chelsea, MI, 1997; pp 397−409.
(4) Haderlein, S. B.; Schwarzenbach, R. P. In *Biodegradation of Nitroaromatic Compounds*; Spain, J. C., Ed.; Plenum: New York, 1995; pp 199−225.
(5) Hering, J. G.; Kreamer, S. In *Perspectives in Environmental Chemistry*; Macalady, D. L., Ed.; Oxford: New York, 1998; pp 57−74.
(6) Macalady, D. L.; Tratnyek, P. G.; Grundl, T. J. *J. Contam. Hydrol.* **1986**, *1*, 1−28.
(7) Tratnyek, P. G.; Macalady, D. L. In *Handbook of Property Estimation Methods for Chemicals: Environmental and Health Sciences*; Mackay, D., Boethling, R. S., Eds.; Lewis: Boca Raton, FL, 2000; pp 383−415.
(8) Amonette, J. E. In *Electrochemistry of Clays*; Fitch, A., Ed.; Clay Minerals Society: Aurora, CO, 2002; 89−147.
(9) Barbash, J. E.; Reinhard, M. In *Biogenic Sulfur in the Environment*; Saltzman, E. S.; Cooper, W. J., Eds.; American Chemical Society: Washington, D.C., 1989; Vol. 393, pp 101−138.
(10) Macalady, D. L.; Ranville, J. F. In *Perspectives in Environmental Chemistry*; Macalady, D. L., Ed.; Oxford: New York, 1998; pp 94−137.
(11) Tratnyek, P. G.; Scherer, M. M.; Johnson, T. J.; Matheson, L. J. In *Chemical Degradation Methods for Wastes and Pollutants: Environmental and Industrial Applications*; Tarr, M. A., Ed.; Marcel Dekker: New York, 2003; pp 371−421.
(12) Arnold, W. A.; Roberts, A. L. *Environ. Sci. Technol.* **2000**, *34*, 1794−1805.
(13) Scherer, M. M.; Johnson, K.; Westall, J. C.; Tratnyek, P. G. *Environ. Sci. Technol.* **2001**, *35*, 2804−2811.
(14) Alowitz, M. J.; Scherer, M. M. *Environ. Sci. Technol.* **2002**, *36*, 299−306.
(15) Tratnyek, P. G.; Reilkoff, T. E.; Lemon, A.; Scherer, M. M.; Balko, B. A.; Feik, L. M.; Henegar, B. *Chem. Educ.* **2001**, *6*, 172−179.
(16) Matheson, L. J.; Tratnyek, P. G. *Environ. Sci. Technol.* **1994**, *28*, 2045−2053.
(17) Harrison, R. J. et al. *NWChem, A Computational Chemistry Package for Parallel Computers*, Ver. 4.0; Pacific Northwest National Laboratory: Richland, WA, 2000.
(18) Frisch, M. J.; et al. *Gaussian 98*, Ver. A.4.; Gaussian, Inc.: Pittsburgh, PA, 1998.
(19) Rassolov, V. A.; Pople, J. A.; Ratner, M. A.; Windus, T. L. *J. Chem. Phys.* **1998**, *109*, 1223−1229.
(20) Hehre, W. J.; Ditchfield, R.; Pople, J. A. *J. Chem. Phys.* **1972**, *56*, 2257−2261.
(21) Dill, J. D.; Pople, J. A. *J. Chem. Phys.* **1975**, *62*, 2921−2923.
(22) Francl, M. M.; Pietro, W. J.; Hehre, W. J.; Binkley, J. S.; Gordon, M. S.; DeFrees, D. J.; Pople, J. A. *J. Chem. Phys.* **1982**, *77*, 3654−3665.
(23) Lee, C.; Yang, W.; Parr, R. G. *Phys. Rev. B* **1988**, *37*, 785−789.
(24) Becke, A. D. *J. Chem. Phys.* **1993**, *98*, 5648−5652.
(25) Godbout, N.; Salahub, D. R.; Andelm, J.; Wimmer, E. *Can. J. Chem.* **1992**, *70*, 560−571.
(26) Klamt, A.; Schüürmann, G. *J. Chem. Soc., Perkin Trans. 2* **1993**, 799−803.
(27) Barone, V.; Cossi, M.; Tomasi, J. *J. Chem. Phys.* **1997**, *107*, 3210−3222.
(28) Wüst, W. F.; Köber, R.; Schlicker, O.; Dahmke, A. *Environ. Sci. Technol.* **1999**, *33*, 4304−4309.
(29) Agrawal, A.; Ferguson, W. J.; Gardner, B. O.; Christ, J. A.; Bandstra, J. Z.; Tratnyek, P. G. *Environ. Sci. Technol.* **2002**, *36*, 4326−4333.
(30) Ritter, K.; Odziemkowski, M. S.; Gillham, R. W. *J. Contam. Hydrol.* **2002**, *55*, 87−111.
(31) Burris, D. R.; Campbell, T. J.; Manoranjan, V. S. *Environ. Sci. Technol.* **1995**, *29*, 2850−2855.
(32) Allen-King, R. M.; Halket, R. M.; Burris, D. R. *Environ. Toxicol. Chem.* **1997**, *16*, 424−429.
(33) Burris, D. R.; Allen-King, R. M.; Manoranjan, V. S.; Campbell, T. J.; Loraine, G. A.; Deng, B. *J. Environ. Eng.* **1998**, *124*, 1012−1019.
(34) Johnson, T. L.; Scherer, M. M.; Tratnyek, P. G. *Environ. Sci. Technol.* **1996**, *30*, 2634−2640.
(35) Gillham, R. W.; O'Hannesin, S. F. *Ground Water* **1994**, *32*, 958−967.
(36) Schreier, C. G.; Reinhard, M. *Chemosphere* **1994**, *29*, 1743−1753.
(37) Campbell, T. J.; Burris, D. R.; Roberts, A. L.; Wells, J. R. *Environ. Toxicol. Chem.* **1997**, *16*, 625−630.
(38) Khudenko, B. M. *J. Environ. Eng.* **1987**, *113*, 681−702.
(39) Ku, Y.; Chen, C.-H. *Separ. Sci. Technol.* **1992**, *27*, 1259−1275.
(40) Kuhn, A. *Met. Finishing* **1993**, *91*, 25−31.
(41) Blowes, D. W.; Ptacek, C. J.; Benner, S. G.; McRae, C. W. T.; Bennett, T. A.; Puls, R. W. *J. Contam. Hydrol.* **2000**, *45*, 123−137.
(42) Pratt, A. R.; Blowes, D. W.; Ptacek, C. J. *Environ. Sci. Technol.* **1997**, *31*, 2492−2498.
(43) Qiu, S. R.; Lai, H. F.; Roberson, M. J.; Hunt, M. L.; Amrhein, C.; Giancarlo, L. C.; Flynn, G. W.; Yarmoff, J. A. *Langmuir* **2000**, *16*, 2230−2236.
(44) Astrup, T.; Stipp, S. L. S.; Christensen, T. H. *Environ. Sci. Technol.* **2000**, *34*, 4163−4168.
(45) Gould, J. P. *Water Res.* **1982**, *16*, 871−877.
(46) Chew, C. F.; Zhang, T. C. *Environ. Eng. Sci.* **1999**, *16*, 389−401.
(47) Huang, C.-P.; Wang, H.-W.; Chiu, P.-C. *Water Res.* **1998**, *32*, 2257−2264.
(48) Cheng, I. F.; Muftikian, R.; Fernando, Q.; Korte, N. *Chemosphere* **1997**, *35*, 2689−2695.
(49) Siantar, D. P.; Schreier, C. G.; Chou, C.-S.; Reinhard, M. *Water Res.* **1996**, *30*, 2315−2322.
(50) Schlicker, O.; Ebert, M.; Fruth, M.; Weidner, M.; Wüst, W.; Dahmke, A. *Ground Water* **2000**, *38*, 403−409.
(51) Hu, H.-Y.; Goto, N.; Fujie, K. *Water Res.* **2001**, *35*, 2789−2793.
(52) Zawaideh, L. I.; Zhang, T. C. *Water Sci. Technol.* **1998**, *38*, 107−115.
(53) Bishop, E. *Indicators*; Pergamon: Oxford, 1972.
(54) Tratnyek, P. G.; Wolfe, N. L. *Environ. Toxicol. Chem.* **1990**, *9*, 289−295.
(55) Tratnyek, P. G.; Macalady, D. L. *J. Agric. Food Chem.* **1989**, *37*, 248−254.
(56) Smolen, J. M.; Weber, E. J.; Tratnyek, P. G. *Environ. Sci. Technol.* **1999**, *33*, 440−445.

(57) Odziemkowski, M. S.; Gui, L.; Gillham, R. W. *Environ. Sci. Technol.* **2000**, *34*, 3495−3500.
(58) Scherer, M. M.; Westall, J. C.; Tratnyek, P. G. *Corros. Sci.* **2001**, *44*, 1151−1157.
(59) Li, T.; Farrell, J. *Environ. Sci. Technol.* **2001**, *35*, 3560−3565.
(60) Khudenko, B. M.; Gould, J. P. *Water Sci. Technol.* **1991**, *24*, 235−246.
(61) Khudenko, B. M. *Water Sci. Technol.* **1991**, *23*, 1873−1881.
(62) Fennelly, J. P.; Roberts, A. L. *Environ. Sci. Technol.* **1998**, *32*, 1980−1988.
(63) Sayles, G. D.; You, G.; Wang, M.; Kupferle, M. J. *Environ. Sci. Technol.* **1997**, *31*, 3448−3454.
(64) Agrawal, A.; Tratnyek, P. G. *Environ. Sci. Technol.* **1996**, *30*, 153−160.
(65) Hundal, L. S.; Singh, J.; Bier, E. L.; Shea, P. J.; Comfort, S. D.; Power, W. L. *Environ. Pollut.* **1997**, *97*, 55−64.
(66) Devlin, J. F.; Klausen, J.; Schwarzenbach, R. P. *Environ. Sci. Technol.* **1998**, *32*, 1941−1947.
(67) Tratnyek, P. G.; Miehr, R.; Bandstra, J. Z. *Groundwater Quality 2001: Third International Conference on Groundwater Quality*; IAHS Press: Sheffield, U.K., 2002; Vol. 275, pp 427−433.
(68) Oh, S. Y.; Cha, D. K.; Kim, B. J.; Chiu, P. *Environ. Toxicol. Chem.* **2002**, *21*, 1384−1389.
(69) Helland, B. R.; Alvarez, P. J. J.; Schnoor, J. L. *J. Hazard. Mater.* **1995**, *41*, 205−216.
(70) Balko, B. A.; Tratnyek, P. G. *J. Phys. Chem. B* **1998**, *102*, 1459−1465.
(71) Scherer, M. M.; Balko, B. A.; Gallagher, D. A.; Tratnyek, P. G. *Environ. Sci. Technol.* **1998**, *32*, 3026−3033.
(72) Scherer, M. M.; Westall, J. C.; Ziomek-Moroz, M.; Tratnyek, P. G. *Environ. Sci. Technol.* **1997**, *31*, 2385−2391.
(73) Roberts, A. L.; Totten, L. A.; Arnold, W. A.; Burris, D. R.; Campbell, T. J. *Environ. Sci. Technol.* **1996**, *30*, 2654−2659.
(74) Tratnyek, P. G. In *Perspectives in Environmental Chemistry*; Macalady, D. L., Ed.; Oxford: New York, 1998; pp 167−194.
(75) Tratnyek, P. G.; Weber, E. J.; Schwarzenbach, R. P. *Environ. Toxicol. Chem.* **2003**, *22*, 1733−1742.
(76) Chen, J.; Pei, J.; Quan, X.; Zhao, Y.; Chen, S.; Schramm, K.-W.; Kettrup, A. *SAR QSAR Environ. Res.* **2002**, *13*, 597−606.
(77) Burrow, P. D.; Aflatooni, K.; Gallup, G. A. *Environ. Sci. Technol.* **2000**, *34*, 3368−3371.
(78) Trohalaki, S.; Pachter, R. *SAR QSAR Environ. Res.* **2003**, *14*, 131−143.
(79) Karelson, M.; Lobanov, V. S.; Katritzky, A. R. *Chem. Rev.* **1996**, *96*, 1027−1043.
(80) Parr, R. G.; Pearson, R. G. *J. Am. Chem. Soc.* **1983**, *105*, 7512−7516.
(81) Parr, R. G.; Zhou, Z. *Acc. Chem. Res.* **1993**, *26*, 256−258.

Received for review March 17, 2003. Revised manuscript received September 19, 2003. Accepted October 6, 2003.

ES034237H